The structural properties of Sn-doped zinc oxide synthesized by hot-tube thermal evaporation

Cite as: AIP Conference Proceedings **1972**, 030005 (2018); https://doi.org/10.1063/1.5041226
Published Online: 05 June 2018

Syahida Suhaimi, Samsudi Sakrani, Nadhrah Md. Yatim, and Mohd Azman Hashim

The Structural Properties of Sn-doped Zinc Oxide Synthesized by Hot-tube Thermal Evaporation

Syahida Suhaimi[1,a)], Samsudi Sakrani[2,b)], Nadhrah Md. Yatim[1,c)] and Mohd Azman Hashim[1,d)]

[1]*Faculty of Science and Technology, Universiti Sains Islam Malaysia, Bandar Baru Nilai, 71800 Nilai, Negeri Sembilan, Malaysia*
[2]*Ibnu Sina Institute, Universiti Teknologi Malaysia, Skudai 81310 Johor Bahru, Johor, Malaysia.*

[a)]Corresponding author: syahida@usim.edu.my
[b)]samsudi3@yahoo.com
[c)]nadhrah@usim.edu.my
[d)]m_azman@usim.edu.my

Abstract. The growth of Sn:ZnO nanowires on a silicon substrate using a low thermal evaporation method is reported. A horizontal quartz tube with controlled supply of O_2 gas were used to fabricate the samples where Zn and Sn metal powders were previously mixed and heated at 500°C. This allows the reactant vapours to deposit onto the substrate, which placed at a certain distance from the source materials. The samples were characterized using FESEM, EDX and HRTEM measurements. Randomly oriented nanowires were formed with varying dopant concentrations from 3 to 15 at%. It was observed that from FESEM images, when the dopant concentrations were increased, a hexagonal rod with a wire extended at its end was clearly formed and the best images of nanowires were shown at the highest concentration of 15 at% measuring between 26 to 35 nm and roughly 500 nm in diameter and length respectively. The doping process played an important role in order to alter the morphological properties of Sn:ZnO nanowires. Sn:ZnO nanowires have large potential in many applications such as in selected sensor technology including gaseous sensors, liquid sensors and others.

INTRODUCTION

Zinc Oxide (ZnO) is a II-IV semiconductor compounds which has a wide bandgap of 3.4 eV. It has a unique features in terms of piezoelectricity and transparent conducting properties that have made it to become a very versatile and promising material. The immense excitement in this area of research arises from understanding the fact that ZnO gives rise to new phenomena and multifunctionality which ultimately leads to unprecedented integration density with nanometer-scale structures [1]. Besides that, it also proposed a high electrical conductivity and optical transmittance in the visible region that make it as an ideal candidate for applications like transparent conducting electrodes in flat panel displays and window layers in solar cells [2]. ZnO become the most preferable material to work in extreme conditions like high power, high temperature and short wavelength for electronic and optoelectronic devices [3]. ZnO has a stable wurtzite structure with lattice spacing a = 0.325 nm and c = 0.521 nm [4]. Doping semiconductor NWs with foreign elements to manipulate their electrical and magnetic properties is an important aspect for the realization of various types of advanced nanodevices [5].

Recent Advancement on Applied Physics, Industrial Chemistry and Chemical Technology
AIP Conf. Proc. 1972, 030005-1–030005-8; https://doi.org/10.1063/1.5041226
Published by AIP Publishing. 978-0-7354-1679-6/$30.00

METHODOLOGY

Materials, Method and Instruments

High purity Zn (99.99%), Sn (99.9%), and oxygen (99.8%) were chosen as the source materials. Silicon is used as a substrate and it must be cleaned to avoid the presence of contaminations and impurities. Si slices were put in a beaker and cleaned in an ultrasonic bath for 30 min at temperature set 40°C with acetone and distilled water. Finally the substrate was dried off with the aid of nitrogen gas blower and stored in a proper desiccator. In the growth process, the growth temperature was set at 650°C and the time taken for the deposition process to complete was 60 minutes. The Sn doped ZnO NWs were obtained by the thermal evaporation method without the presence of catalysts. The reaction system was well controlled by adjusting the parameters of temperature, carrier gas flow rate, growth reaction time and concentration of dopants. Synthesize by thermal evaporation requires quartz tube which is open on both sides, one of the open side iss connected to the pump while the other one is used as inlet for carrier gas which connected to the gas supply. Quartz tube was placed inside a furnace source and substrate materials set inside the quartz tube. Source material was held at the inlet side while substrate material was held on the other side horizontally. Inside the tube, the source temperature was set to be higher than the substrate temperature.

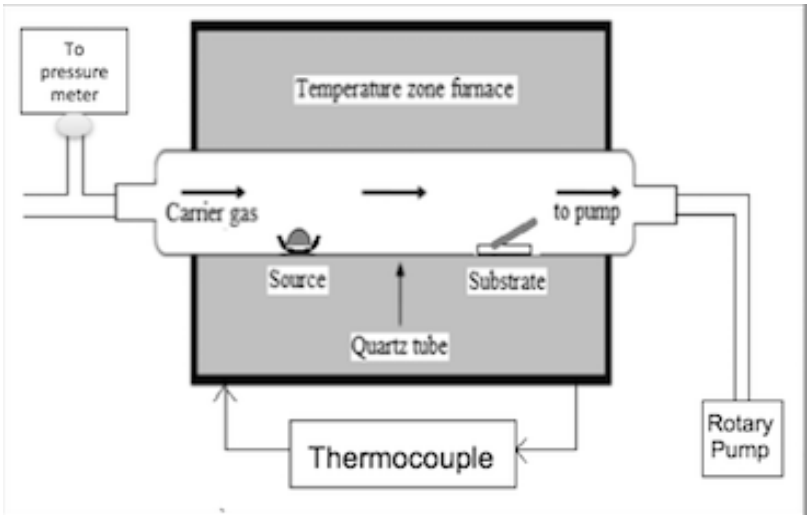

FIGURE 1. Schematic of the main system for experimental setup.

The preparation of ZnO nanowires by evaporating the metallic component had been achieved in the presence of inert gas (Argon) so that a nanometer-sized was obtained. The loose metallic powder was subsequently oxidized by introducing air or oxygen into the chamber at different annealing temperatures of zinc metal. However in the present study, Zn powder is evaporated directly using an electrical furnace as evaporation source with air flow-rate pressure. The nanosized ZnO particles produced by evaporating method can be applied to wide range of nanomaterials systems. Sternum (Sn) which also known as tin is one dopant that can be used to change the composition of the resulting nanocrystals but also influenced the growth of host lattices [6].

Doping Mechanism of ZnO:Sn

Doping is an effective approach to modify the properties of nanocrytals by tailoring the composition of the crystals. A few recent studies found that doped ZnO nanowires will proposed better electrical conduction at higher temperature supplied [7]. The emission for photoluminescence spectra can be controlled by the flow rate of the gas. Our group is interested in the doping and shape control of the nanowires because ZnO is a technologically important and environmentally friendly wide band-gap semiconductor with many unique properties. In the previous study, we

have demonstrated the synthesis of Al-doped ZnO (ZnO:Zn) nanowires with well-define shapes measuring between 260 to 350 nm and 720 nm in diameter and length, respectively. These nanowires exhibits a strong UV emission band located at approximately 389 nm (E_g = 3.19 eV) with other low intensity peaks at wavelength greater than 400 nm which contributed by oxygen vacancies. In addition to Zn^{2+}, a group III metal ion, preliminary results showed that the introduction of Al^{3+} influences the shapes of the resulting doped ZnO nanocrystals. Inspired by these findings, we proposed that dopants of group IV ions may have similar effects on the shapes of the doped ZnO nanowires. Furthermore, we hypothesized that the dopant concentration of Sn does played an important role in changing the structural and optical properties of ZnO nanostructures.

In this study, we employ the synthesis of Sn-doped ZnO nanowires as an example to verify the above hypothesis. The morphological, structural, and optical properties were characterized by FESEM, HRTEM, PL and XRD.

Vapor-Liquid-Solid (V-L-S) and Vapor-Solid (V-S) Mechanisms

The vapor-liquid-solid (VLS) and Vapor-Solid (VS) formation mechanisms are usually responsible for the 1-dimensional (1-D) semiconductor nanowires. For the VLS mechanism, the metal nanoclusters act as catalyst and guide the nanowire to grow towards the 1-D direction. There is evident that the nanowire tip will have an alloy droplet.

In this experiment, no impurity metal particles were detected in the ZnO nanowires. Therefore, we can conclude that the V-S growth process is applicable in this process. At the early stage of the growth process, a reaction occurs between Zn and O_2 to form ZnO_x (x>1); the ZnO_x vapor is transferred by the O_2 to the nuclei at the Si substrate. The continuous supply of O_2 will eventually oxidized ZnO_x to ZnO. The highly supersaturated Zn, ZnO_x vapor and oxygen will assist the ZnO nanostructures to nucleate easily and grow along the [0001] direction, which was substantiated by the HRTEM image as shown in Fig. 4. The already-formed ZnO nucleation continues to grow along the direction of the O_2 gas flow in order to allow the formation of some well-aligned ZnO nanowires on the Si substrate.

Alloying evaporation method

According to the self-catalytic growth mechanism proposed by Dang et al. [8], the process completes in four major steps. Figure 2 best explains the particular growth mechanism. It can be understood as follows: (A) as soon as the furnace temperature reaches the melting point of the Zn powder, it starts to melt and form a large quantity of melting liquid drops of size approximately identical to those of the original solid metal particles. (B) The oxygen in the inlet flow is then absorbed by the melting metal at some points on the surface resulting in some metal oxide nanoclusters, which serve as nuclei for the nanowire growth. (C) Depending on the availability of source metal reactants and appropriate quantities of O_2, the growth of metal oxide NWs begins and continues after the formation of the nuclei. (D) Growth of ZnO NWs terminates when the source metal is exhausted. Figure 2 shows the step taken during the growth of ZnO NWs using thermal evaporation technique.

The atomic ratio of Zn:O on the tip and root of a NR was not the same. Concentration of oxygen at the tip of the ZnO NRs exceeded the root [9]. The fact is attributed to the alloying of Sn/Zn mixed sources during the growth of NRs. The Sn vapor pressure is much lower than that of Zn at the same temperature range. However, Zn and Sn sources in the process would form a certain quantity of Zn-Sn alloy by interdiffusion through the Zn/Sn interface. Since the bond energy of Zn-Sn, 0.201 eV, is higher than that of Zn-Zn, 0.054 eV, which may cause the decreasing of Zn vapor pressure in the quartz tube with the alloying of Zn and Sn during the deposition process. On the other hand, the flow rate of oxygen in the furnace is kept constant. As a result, the tip of Sn:ZnO NWs exhibits lower zinc concentration than the root. This particular process has contributed to unique optical properties of the NWs as described below. With higher zinc and lower oxygen concentration at the root of NWs, it reflects green emission that is attributed to the existence of oxygen vacancy.

RESULTS AND DISCUSSION

Synthesis ZnO:Sn Nanowires

The experimental results of ZnO:Sn NWs grown from alloying evaporation deposition (AED) growth mechanism using themal evaporation technique are illustrated. Thermal evaporation is very sensitive to any

parameter changes such as dopant concentration, furnace temperature, growth time, gas flow rate and substrate holder's angel. This paper discusses the effect of dopant concentration on both structural and optical properties of grown nanowires and how the optimum value for the chosen parameter was identified. The growth parameters of Sn:ZnO NWs are presented in Table 1 as follow.

TABLE 1. Variation of Dopant Concentration on Sn:ZnO Growth Process.

Sample Name	Sn Dopant Concentration (at%)	Temperature (°C)	Growth Time (min)
Sn:ZnO 1	3	650	60
Sn:ZnO 2	9	650	60
Sn:ZnO 3	15	650	60

However, we have narrowed down and decided to focus our study mainly on the effects of dopant concentrations keeping the rest of the parameters invariant. Different samples with various dopant concentrations were analyzed using field emission scanning electron microscopy (FESEM), high-resolution transmission electron microscopy (HRTEM), energy-dispersive analisis x-ray (EDAX) and photoluminescence (PL) and the results obtained are interpreted in the following sections.

Effect of Dopant Concentration on ZnO:Sn Nanostructure

Different concentration of dopant could affect much on the structural properties of Sn:ZnO nanowires especially in its size and shape [10]. At the beginning of the analysis stage, the formation and existence of ZnO NWs were done by attaining the images from basic scanning electron microscopy (SEM) technique. Figure 2 shows the early findings where ZnO NWs appeared as a bushy mesh that extends its diameter for about 30 nm in average. It is immense assurance that the experimental setup is impressive and capable of producing NWs with such incredible dimensions.

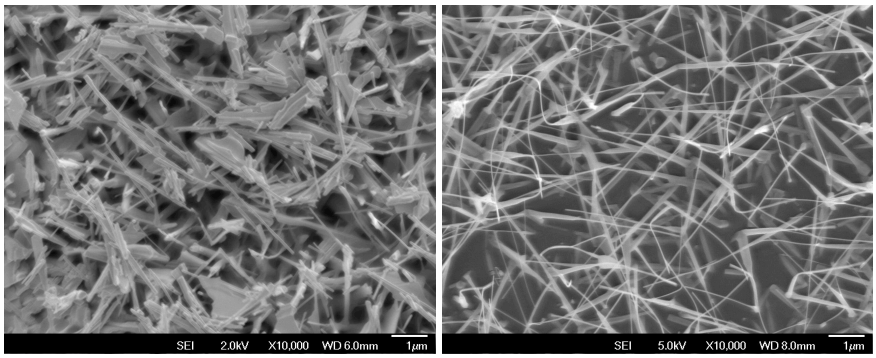

FIGURE 2. FESEM images of undoped and doped ZnO nanowires.

Structural Properties of ZnO:Sn Nanowires

The FESEM images in Figure 2 indicate that ZnO NWs are randomly oriented. The vapor-liquid-solid (VLS) and vapor-solid (VS) formation mechanisms are usually responsible for the 1-D semiconductor nanowires. FESEM analysis was used to charactize the nucleation and growth during the early stages (doped and undoped) ZnO nanowires to better understand the effect of the first Sn dopant formation on ZnO. ZnO nanowires were prepared by thermal oxidation technique and the resulting products were investigated by several electron microscopic techniques including FESEM and TEM for morphology and lattice spacing measurements. Figure 2 illustrated the comparison between undoped ZnO nanowire (pure) and doped ZnO nanowires (Sn:ZnO). A uniform long and thin Sn:ZnO nanowires with average diameter of 25 nm and several microns in lengths was succesfully grown with the presence

of Sn dopant. It is of immense that the experimental set-up is impressive and capable of forming nanowires. TEM was used to further characterize the single ZnO nanowires for their lattice spacing, directions and plane. The Sn:ZnO nanowires grown on the Si wafer were torn off from the substrate using a ulrasonic machine for its vibrating mechanisms and transferred to a copper grid.

Different morphologies of the sample products can be seen in Fig. 3. The concentration of Sn dopant being introduced into the process play an important parameter in controlling morphology of sommewhat wire-like and belt-like nanostructures [11]. From the images, it can be clearly observed that the growth of high density ZnO nanowires on Si (100) bulk substrates was not achieved at all tested dopant concentrations. In Fig. 3(a) for example, the grown ZnO nanostructures were non-uniform and sparsely distributed on the entire substrate. The nucleation of Zn and ZnO_x seeds as well as the subsequent growth of ZnO nanowires on the bare Si substrate seem to be difficult with the present growth parameter due to the large lattice mismatch between ZnO and Si [12].In this result the shape of nanowires depend on the concentration of Sn dopant in the quartz tube as tabulated in Table 1. FESEM images in Fig. 3 composed of Sn:ZnO nanowires with perfectly hexagonal-shaped and uniform in its diameter which belongs to the lowest dopant concentration. As the concentration was increased, the nanostructures changed to tetrapod nanowires with hexagonal cylinder legs that sized slightly bigger than those three nanowire emerged from it. The leg has a length of around 60 nm and as can be seen in the figure the formation of this kind of nanowires is not as good as the previous set where the substrate area is not fully covered by the grown nanowires or tetrapods. The formation of tetrapods nanowire was further discussed by Zhou Z. et. Al [13]. It is worth noting that higher dopant concentration has helped in providing appropriate surfaces or planes for Zn or ZnO_x seed nucleation at the initial stage so that the subsequent growth of Zn nanowires can be promoted. It is obvious that Sn:ZnO nanowires growth become prominent at 15 at% of Sn dopant. Energy dispersive x-ray spectroscopy (EDX) was used to identify the component elements of the NWs. Several materials were detected as can be seen in Fig. 4.

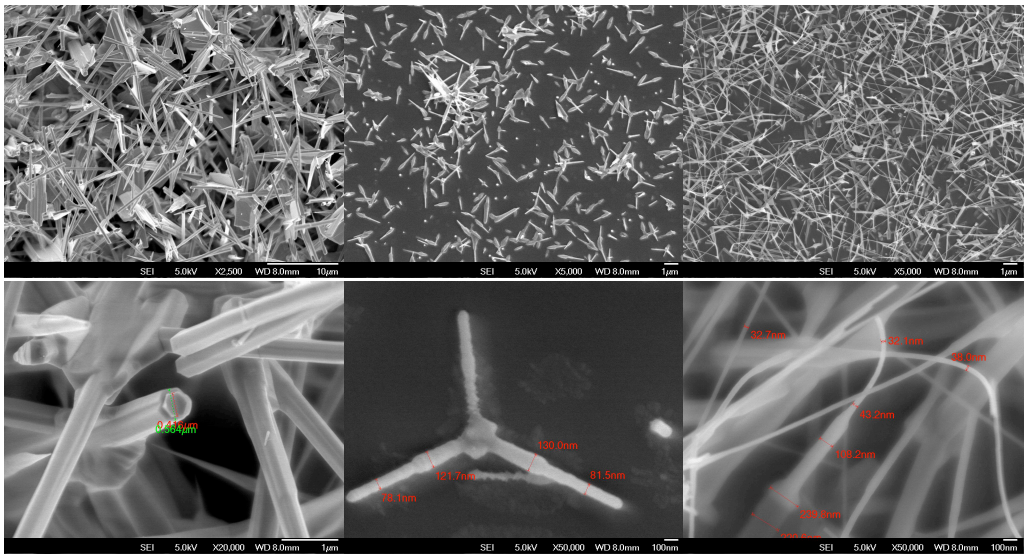

FIGURE 3. Sn doped ZnO nanowires at a) 3 at% Sn b) 9 at% Sn and c) 15 at% Sn at two different magnification.

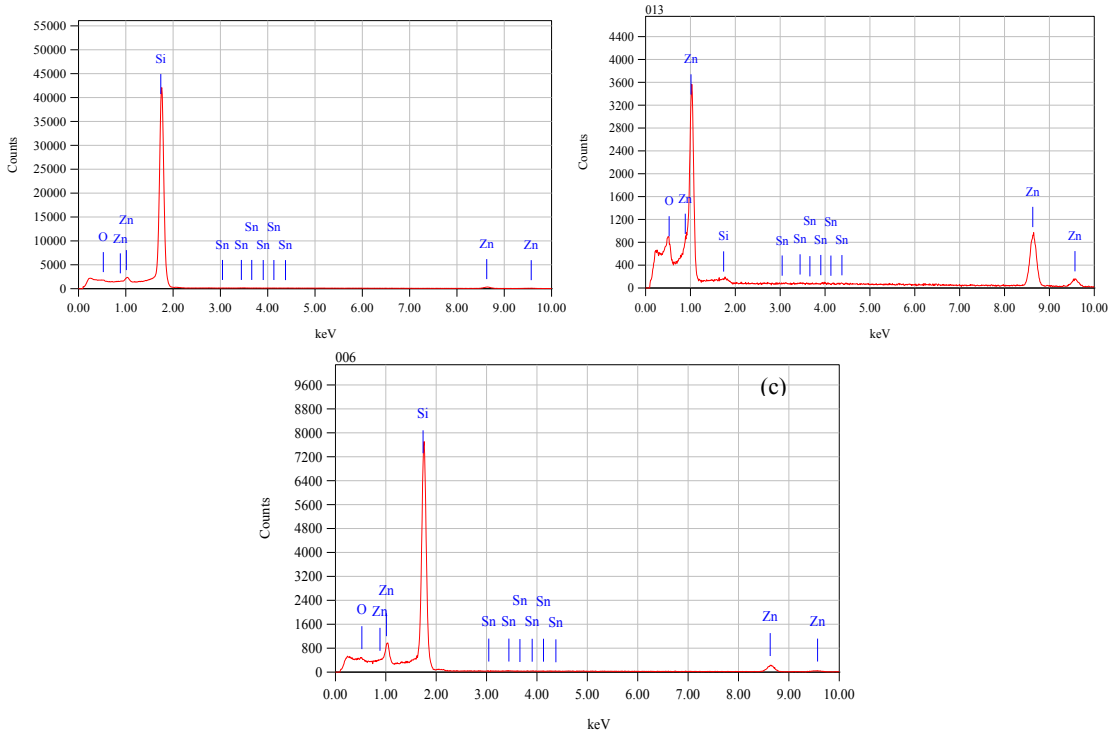

FIGURE 4. EDX spectrum recorded at different dopant concentrations of the ZnO nanowires. Picture (a) is 3 at% Sn:ZnO, (b) is 9 at% Sn:ZnO and (c) 15 at% Sn:ZnO nanowires.

Spectrum (a) shows the EDX analysis recorded at the dopant concentration of 3 at%, 9 at% Sn:ZnO nanowires formed a tripod shapes as shown in (b) and the highest concentration which is the best parameter to be pointed is 15 at% Sn:ZnO as in Figure 4 (c). From the spectrums, elements C probably comes from the TMGa, Si peaks arised just from the substrate material. While O a from exposure to the air because the moment it took out from the reactor, it is exposed to atmosphere. Pt is detected due to the sample coated before EDX process. It is found that from the spectrums, a large quantity of Zn and O were observed nearly 80% of the materials contain on each of nanowires. The Zn and O peaks also reached the highest peak compare to others materials. Nanowire has very large surface area; therefore the Sn peak is very small compare to Zn and O.

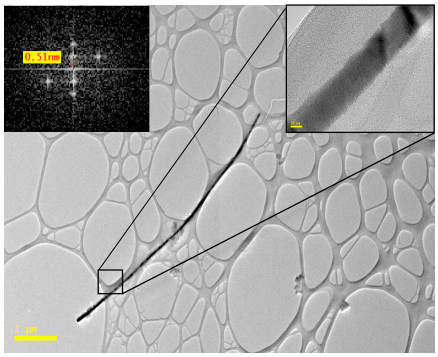

FIGURE 5. HRTEM images of synthesized Sn:ZnO nanowire at 15 at% dopant concentration.

Figure 5 shows HRTEM image for the Sn-doped ZnO nanowire dispersed on the copper grid for singly-nanowire measurement purposes. As presented in above figure, a very long and thin nanowire was lied on the grid. As mentioned before, the nanowires have the diameter in the range of 25-35 nm and the FFT pattern indicates that the nanowires are consisted of nearly single-crystalline wurtzite ZnO crystal with the [001] growth direction. The (001)

fringes separated by 0.51 nm and are parallel to the growth direction. The length of the nanowire approximately about 0.3 micron where we can see from the HRTEM analysis that several nanowires were captured having a length more than 0.4 micron as well.

The higher magnification image of Sn:ZnO nanowires can be seen in Figure 5 which shows HRTEM image of the prepared nanowire with a uniform diameter of 26 nm. The as-prepared doped ZnO nanowire was further analyzed with HRTEM special measurement equipment and the measured spacing of lattice fringes is 0.51 nm, corresponding to the d-spacing of the (0001) planes of wurtzite ZnO. Based on the HRTEM image of the nanowire, no stacking faults and dislocations are observed. This reveals the well-crystalline nature of ZnO nanowire. In this particular work, highly crystalline ZnO nanowires are synthesized in the absence of a catalyst.

The Sn-assisted growth of ZnO nanowires has such impacts on the formation of longer and thinner nanowires. The Sn in the alloy dropletscan diffuse into ZnO nanowires through thermal process. The content of Sn in the Sn:ZnO nanowires can be measured by EDX spectra which has been conducted along with FESEM analysis earlier. This indicates that the fraction of Sn to Zn can influence the morphologies of the Sn doped ZnO nanowires. The HR-TEM images of the Sn:ZnO nanowires depict the effect of doping on the lattice system. The clear lattice fringes of (0002) planes of Sn:ZnO nanowires are indicated in Fig. 5 inset image .

CONCLUSION

Dopant plays an important role on controlling the morphology of ZnO NWs. As evident from the result, it indicates that the optimum dopant concentration to be at 15 at% of Sn where a 'syringe-like' nanowire were formed. We also obtained very interesting nanostructures at 3 at% which appear a definite hexagonal shaped nanowire but in a short length formation. We assume 15 at% to be an optimum dopant concentration necessary which resulted in the formation of very long and thin nanowires. From SEM, FESEM and HRTEM, we felt that the doping mechanism occurs via formation of oxygen vacancies (V_o) and zinc interstitials (Zn_i) rather than substitution as in the case for conventional methods.

ACKNOWLEDGEMENT

The authors thank the Department of Physics, Faculty of Science and Ibnu Sina Institute, Universiti Teknologi Malaysia, Johor, for all facilities provided as well as to Malaysian Government (FRGS) under vote 4F322 for funding the project.

REFERENCES

1. A. K. Singh and R. Kishan, "Comparative Study of Zinc Oxide Nanostructures Synthesized by Oxidation of Zinc Foil and Zinc Powder", Ph.D. thesis, National Institute of Technology, Rourkela, 2011.
2. M. Kumar and S. S. Sahu, "Zinc Oxide Nanostructures Synthesized by Oxidation of Zinc", Ph.D. thesis, National Institute of Technology, Rourkela, 2010.
3. X. Zhai, Y. Fu, B. Lu, B. Bai and J. Wang, Nanoscience **11** (3), 161-167 (2006).
4. Z. Fan and J. G. Lu, "Zinc Oxide Nanostructures: Synthesis and Properties", Ph.D. thesis, University of California, Irvine, California, 2005.
5. L. J. Lauhon, M. S. Gudiksen and C. M. Lieber, Semiconductor Nanowire Heterostructures; Philosophical Transactions of the Royal Society of London, Series A: Mathematical and Physical Science, Philos. Trans. R. Soc. Lond. **362**, 1247-1260 (2004).
6. N. Wang, Y. Cai and R. Q. Zhang, Growth of Nanowires, Materials Science and Engineering **60**, 1-51 (2008).
7. Y. L. Seu, L. Pang, Y. L. Chia, Y. T. Tseung and J. H. Chorng, J. Phys. D: Appl. Phys. **37**, 2274-2282 (2004).
8. H. Y. Dang, J. Wang and S. S. Fan, Nanotechnology **14**, 738-741 (2003).
9. C. P. Liu, Multi-Channel ZnO Nanoconductors with Tunable Opto-Electrical Properties. Available from Final Report of the Air Force Project (FA4869-06-0078), Tainan, Taiwan: National Cheng Kung University, (2007).
10. Q. Wan, S. Jia and H. Liu, Semiconducting Oxides Nanowires, Nanowires; Implementation and Application, Ningbo Institute of Materials Technology and Engineering, Hunan University, China.
11. Z. R. Dai, Z. W. Pan and Z. L. Wang, Novel Nanostructures of Functional Oxides Synthesized by Thermal Evaporation, Adv. Funct. Mater. **13**, 9-24 (2003).

12. N. I. Rusli, M. Tanikawa, M. R. Mahmood, K. Yasui and A. M. Hashim, Growth of High-Density Zinc Oxide Nanorods on Porous Silicon by Thermal Evaporation, Materials **5**, 2817-2832 (2012).
13. Z. Zhou, W. Peng, S. Ke and H. Deng, Tetrapod-shaped ZnO Whisker and Its Composites, J. Mater. Process. Technol **89-90**, 415-418 (1999).